Analysis of Phase-Boundary Motion in Diffusion-Controlled Processes:

Part III. Penetration of Metal Ions into Cellulose Xanthate Fibers and Growth of Sulfuric Acid Droplets in Humid Air

J. R. GRIFFIN and D. R. COUGHANOWR

Purdue University, Lafayette, Indiana

In Part I (1) three general methods of solving moving-boundary problems were developed, and in Part II (2) the three methods were applied to the problem of evaporation from a flat surface into a gas of infinite depth. In this final paper, more challenging problems in cylindrical and spherical coordinates are considered, and new solutions to these are presented.

PENETRATION OF METAL IONS INTO CELLULOSE XANTHATE FIBERS

Description of Problem

Hermans (3) has described some experiments and an attempted theoretical treatment of the diffusion and reaction of copper ions in filaments of cellulose xanthate. The type of problem encountered, a typical moving-boundary problem, aroused interest in several quarters. Hermans (4) has discussed the generality of this phenomenon as applied to the swelling and shrinking of polymers,* and Fujita (5) has recalculated the data presented by Hermans (3) according to an approximation procedure known as the method of moments in an attempt to obtain a more satisfactory explanation of the data. The problem, involving radial diffusion-controlled boundary motion in a finite medium, remains unsolved to the knowledge of the authors.

The copper ions react with the cellulose xanthate instantaneously, one copper ion reacting with two CS_2 groups. The CS_2 groups are fixed in the structure of the filament, so that the copper ions must diffuse radially inward as the CS_2 is neutralized near the surface. A sharp boundary surface may be observed to penetrate toward the center of the filament as the process proceeds; the reacted portion of the filamenet is dark brown in color, while the unreacted portion is orange. The reaction surface is located at the radial position where the concentration of copper ions is zero. The concentration of copper ions at the surface of the filament is maintained constant by agitation of the copper solution.

Since there is no convection in the filament, the quiescent phase procedure developed in (1) applies, and the differential equation is as follows:†

$$D\left(\frac{\partial^2 c}{\partial r^2}+\frac{1}{r}\frac{\partial c}{\partial r}\right)=\frac{\partial c}{\partial t}, \qquad R(t)\leq r\leq R_o \quad (1)$$

where $R(t)$ is the radial position of the reaction surface and R_o is the radius of the filament. The initial condition for c is immaterial, since the diffusion zone is initially of zero dimenson. At the reaction surface

$$c(R,t)=0 \quad (2)$$

while at the surface of the cylinder

$$c(R_o,t)=a=\text{constant} \quad (3)$$

A material balance for copper ion at the reaction surface yields

$$D\frac{\partial c}{\partial r}(R,t)=-\frac{1}{2}b\dot{R} \quad (4)$$

The problem may be cast into a more convenient form by defining the following dimensionless variables:

$$s=r/R_o \quad (5)$$

$$\theta=Dt/R_o^2 \quad (6)$$

$$B=R/R_o \quad (7)$$

$$u=c/a \quad (8)$$

The problem then becomes

$$\frac{\partial^2 u}{\partial s^2}+\frac{1}{s}\frac{\partial u}{\partial s}=\frac{\partial u}{\partial \theta} \qquad B\leq s\leq 1 \quad (9)$$

J. R. Griffin is with the Humble Oil and Refining Company, Baytown, Texas. D. R. Coughanowr is currently on sabbatical leave at the Swiss Federal Institute of Technology in Zurich, Switzerland.

* This work includes some interesting microphotographs of the type of phenomena considered here.

† The formulation of this problem in terms of a simple diffusion mechanism with constant diffusivity and density and neglect of the effects of the ionic charges may well be questioned. However, Hermans (3) found that such a model was adequate to describe the mass transfer in linear flow experiments on the same system. It is therefore felt that his difficulties stemmed from mathematical problems in solving the model, rather than in the model itself.

$$u(B, \theta) = 0 \tag{10}$$

$$u(1, \theta) = 1 \tag{11}$$

$$\frac{\partial u}{\partial s}(B, \theta) = \frac{b}{2a}\dot{B} \tag{12}$$

Solution

The auxiliary problem corresponding to Equations (I.19) through (I.24)* is

$$\frac{\partial^2 v}{\partial s'^2} + \frac{1}{s'}\frac{\partial v}{\partial s'} = \frac{\partial v}{\partial(\theta - \theta')} \tag{13}$$

$$v(s', 0) = 0, \quad s' \neq s \tag{14}$$

$$v(s, 0) = \infty \tag{15}$$

$$\lim_{\epsilon \to 0} \int_{s-\epsilon}^{s+\epsilon} 2\pi s'\, v(s'. 0)\, ds' = 1 \tag{16}$$

$$v(1, \theta - \theta') = 0 \tag{17}$$

$$v(0, \theta - \theta') = 0 \tag{18}$$

This auxiliary problem is readily solved by Laplace transformation with respect to $(\theta - \theta')$ to give the following result:

$$v = \frac{1}{\pi}\sum_{n=1}^{\infty} \frac{J_0(\lambda_n s) J_0(\lambda_n s')}{[J_1(\lambda_n)]^2} \exp - [\lambda_n^2(\theta - \theta')] \tag{19}$$

where the λ_n are eigenvalues, $0 < \lambda_1 < \lambda_2 \ldots$, which are the roots of

$$J_0(\lambda) = 0 \tag{20}$$

The boundary equations, corresponding to Equations (I.7) and (I.13) are as follows. On the moving boundary

$$0 + F_{B'}\frac{b}{2a}\dot{B}' = G_{B'} \tag{21}$$

from which†

$$\left(\frac{vG}{F}\right)_{B'} = v_{B'}\frac{b}{2a}\dot{B}' \tag{22}$$

For the fixed boundary, on the other hand, Equation (I.7) corresponds to

$$1 + F_1\left(\frac{\partial u}{\partial s}\right)_1 = G_1 \tag{23}$$

and since the gradient at the fixed boundary is not known, one may put

$$F_1 = 0; \qquad G_1 = 1 \tag{24}$$

From Equation (I.13) then

$$v_1 = 0; \qquad (v/F)_1 = -\left(\frac{\partial v}{\partial s'}\right)_1 \tag{25}$$

so that

$$\left(\frac{vG}{F}\right)_1 = -\left(\frac{\partial v}{\partial s'}\right)_1 \tag{26}$$

Evaluating Equations (22) and (26) using Equation (19), one writes the solution according to Equation (I.14) as follows:

$$u = \int_0^\theta 2\sum_{n=1}^{\infty} \frac{b}{2a}\frac{J_0(\lambda_n s) J_0(\lambda_n B')}{[J_1(\lambda_n)]^2} B'\dot{B}' \exp - [\lambda_n^2(\theta - \theta')]d\theta' + \int_0^\theta 2\sum_{n=1}^{\infty} \frac{\lambda_n J_0(\lambda_n s)}{J_1(\lambda_n)} \exp - [\lambda_n^2(\theta - \theta')]d\theta' \tag{27}$$

Integrating the second term in Equation (27), noting the Fourier-Bessel expansion of unity in the unit interval, and performing an integration by parts in order to eliminate the boundary velocity, one may write the solution in terms of the original variables as follows:

$$\frac{c}{a} = 1 - 2\left(1 + \frac{b}{2a}\right)\sum_{n=1}^{\infty} \frac{J_0(\lambda_n r/R_0)}{\lambda_n J_1(\lambda_n)} \exp - (\lambda_n^2 Dt/R_0^2) + \frac{b}{a}\sum_{n=1}^{\infty} \frac{J_0(\lambda_n r/R_0)}{\lambda_n J_1(\lambda_n)} \frac{R}{R_0}\frac{J_1(\lambda_n R/R_0)}{J_1(\lambda_n)} - \frac{\lambda_n^2 D}{R_0^2}$$
$$\int_0^t \frac{R'}{R_0}\frac{J_1(\lambda_n R'/R_0)}{J_1(\lambda_n)} \exp - [\lambda_n^2 D(t - t')/R_0^2]dt' \tag{28}$$

The Boundary Motion

An equation for the moving boundary may be obtained in any of several forms by applying some variant of the conditions to be met there. In terms of the present problem, these conditions are given by Equations (2) and (4). Two equations which must be satisfied by $R(t)$ may therefore be written immediately from Equation (28):

$$1 = 2\left(1 + \frac{b}{2a}\right)\sum_{n=1}^{\infty} \frac{J_0(\lambda_n R/R_0)}{\lambda_n J_1(\lambda_n)} \exp - (\lambda_n^2 Dt/R_0^2) + \frac{b}{a}\sum_{n=1}^{\infty} \frac{J_0(\lambda_n R/R_0)}{\lambda_n J_1(\lambda_n)} \phi_n \tag{29}$$

and

$$\frac{bR_0}{2aD}\frac{dR}{dt} = -2\left(1 + \frac{b}{2a}\right)\sum_{n=1}^{\infty} \frac{J_1(\lambda_n R/R_0)}{J_1(\lambda_n)} \exp - (\lambda_n^2 Dt/R_0^2) - \frac{b}{a}\sum_{n=1}^{\infty} \frac{J_1(\lambda_n R/R_0)}{J_1(\lambda_n)} \phi_n \tag{30}$$

where

$$\phi_n(R, R_0, D\,t, \lambda_n) = \frac{\lambda_n^2 D}{R_0^2}\int_0^t \frac{R'}{R_0}\frac{J_1(\lambda_n R'/R_0)}{J_1(\lambda_n)} \exp - \left[\frac{\lambda_n^2 D(t - t')}{R_0^2}\right]dt' - \frac{R}{R_0}\frac{J_1(\lambda_n R/R_0)}{J_1(\lambda_n)} \tag{31}$$

By virtue of the negative exponential terms, the series in Equations (29) and (30) are rapidly convergent for large times. For sufficiently large times a first-term solution of both Equations (29) and (30) will be adequate. In this case, a remarkably simple boundary equation emerges by dividing Equation (29) into (30):

$$\frac{R_0 b}{2aD}\frac{dR}{dt} \doteq -\frac{\lambda_1 J_1(\lambda_1 R/R_0)}{J_0(\lambda_1 R/R_0)} \tag{32}$$

When a single-term solution will simply not do, the situation, while considerably darkened, is not an impossible one. Solution of Equation (29) is not at all attractive, but Equation (30) is a Volterra equation of the second kind and is thus subject to solution by iteration.

In analyzing the experimental data of Hermans (3) (see below), it was desirable to perform such a multiple-term calculation for one set of conditions. As a starting ap-

* The Roman numeral preceding an equation number refers to an equation in part I of this series (1).

† The equation corresponding to Equation (I.13) is not needed when u is zero on the boundary.

proximation, the opportunity was taken to introduce the quasi steady model for the process*.

$$\frac{Dt}{R_o^2} = \frac{b}{8a}\left[\left(\frac{R}{R_o}\right)^2 [\ln (R/R_o)^2 - 1] + 1\right] \quad (33)$$

Comparison with Other Solutions and Data

Hermans (3) has presented data on the time required for the reaction surface to penetrate halfway to the center of the filament. To facilitate the discussion, these data, along with several other quantities which shall be of interest shortly, are reproduced in Table 1.

The experimentally determined constant k is that which appears in the following empirical equation used by Hermans:

$$R_o - R = k\,(\sqrt{t} + \sqrt{T} - \sqrt{T - t}) \quad (34)$$

Hermans observed that while Equation (34) failed to represent his data adequately for $R \doteq R_o$ and again for $R \doteq 0$, it was quite satisfactory in the neighborhood of $R = R_o/2$, and that in fact $R = R_o/2$ when $t = T/2$. The measured values of R_o and $T/2$ are thus related by

$$k = R_o/2\sqrt{T} \quad (35)$$

An alternate form of this quantity may be obtained by eliminating T between Equation (34) and its time derivative for $t = T/2$:

$$k^2 = -\frac{R_o}{2\sqrt{2}}\left(\frac{dR}{dt}\right)_{T/2} \quad (36)$$

To compute the diffusion coefficient, Hermans noted that in accordance with Equation (34) for small t one has

$$R_o - R \doteq k\sqrt{t} \quad (37)$$

which is the same form as can be obtained on theoretical grounds for the case of penetration of a plane boundary. This theory is closely related to that considered in Part II (2), and the solutions are analogous to Equations (II.50) and (II.52), for $\epsilon = 0$. On this basis, Hermans computed values of D from his experimental data. These are shown in Table 1.

Hermans also measured D directly by the well-known steady state method (diffusion through a slab) and obtained a value of $(1.6 \pm 0.3) \times 10^{-6}$ sq. cm./sec., thus discrediting his own attempted theoretical development.

Fujita (5) recalculated the data in accordance with an approximation scheme known as the *method of moments,* which must be described as tedious. The results of Fujita's calculations are presented in Table 1, beside those of Hermans. Fujita concluded his paper with the remark: "The appreciable discrepancy here again revealed for the cylindrical case is yet not clear to us, although it may in part be due to some insufficient or incorrect approximation in the mathematical solution obtained."

It will not be the goal here to make a precise calculation of the diffusion coefficient but rather to show, by means of the present theory, that the cylindrical data of Hermans are quite consistent with a diffusion coefficient as found by his steady state measurements, as opposed to such as were calculated by him and by Fujita. Thus, Equations (32) and (36) may be combined to provide the relationship

$$k^2 = \frac{\lambda_1}{\sqrt{2}}\frac{J_1(\lambda_1/2)}{J_0(\lambda_1/2)} D \frac{a}{b} \quad (38)$$

which, being a one-term solution, may be expected to apply asymptotically for large diffusion times. Large diffusion times for a given degree of penetration will be realized for small values of (a/b), an infinite time being required for any degree of penetration as (a/b) approaches zero. Thus $k = 0$ for $(a/b) = 0$ is a physical condition which must be realized.

Table 1. Data of Hermans with Calculated Diffusivities of Hermans and of Fujita

Run	a	b	$k \times 10^3$	$D_H \times 10^6$	$D_F \times 10^6$
1	0.40	0.126	1.65	0.54	—
2	0.20	0.126	1.35	0.53	1.39
3	0.133	0.126	1.08	0.44	1.17
4	0.10	0.126	0.98	0.45	1.17
5	0.05	0.126	0.72	0.41	1.02
6	0.025	0.126	0.53	0.41	0.90
7	0.018	0.126	0.47	0.43	0.93
8	0.20	0.330	0.83	0.40	1.00
9	0.20	0.270	0.86	0.37	0.97
10	0.20	0.250	0.90	0.38	0.97
11	0.20	0.190	1.05	0.41	1.10
12	0.20	0.190	1.09	0.44	1.19
13	0.20	0.130	1.19	0.42	1.14

a = copper ion concentration, g.-moles/liter.
b = xanthate concentration, g.-moles/liter.
k = Hermans' experimental quantity, Equation (34), cm./sec.
D_H = diffusion coefficient as computed by Hermans, sq. cm./sec.
D_F = diffusion coefficient as computed by Fujita, sq. cm./sec.

In view of this, one may plot Hermans' data as k^2 vs. (a/b) for several of his runs corresponding to low values of (a/b) and extrapolate the curve defined so as to make it pass through the point $(0, 0)$. This done, the slope of the curve so obtained at $(0, 0)$ should be related to the diffusion coefficient by the following expression which comes from Equation (38):

$$\text{Slope at origin} = \frac{\lambda_1}{\sqrt{2}}\frac{J_1(\lambda_1/2)}{J_0(\lambda_1/2)} D \quad (39)$$

Hermans' four runs which have the lowest values of the ratio (a/b) are runs number four, five, six, and seven. It happens that these runs are for a constant value of $b = 0.126$, so that when k^2 is plotted vs. the copper ion concentration, a, one should have

$$\text{Slope} = \frac{\lambda_1 J_1(\lambda_1/2) D}{\sqrt{2}(0.126) J_0(\lambda_1/2)} = \frac{(2.40) J_1(1.20) D}{(1.41)(0.126) J_0(1.20)} = 10.0\, D \quad (40)$$

The results of this procedure are shown in Figure 1, where a line through the origin with a slope for $D = 1.6 \times 10^{-6}$ has been superimposed for convenience. It is clear from Figure 1 that the data of Hermans are consistent with a diffusion coefficient in the range found by him in the steady state slab, and that they do not indicate a diffusion coefficient as low as those computed by Hermans or by Fujita.

It was considered desirable to perform a multiple-term calculation by hand, as described earlier, in order to gain an appreciation of what might be encountered in a calculation of this sort. These calculations are obviously tedious and involved when so performed, and only one iteration was made.† Apart from indicating that nothing unforeseen occurs, the results are of interest and are presented in Figure 2. While two terms were found adequate for the conditions assumed (run number seven), four terms were carried throughout.

In addition to the initial approximation [Equation (33)] and the first iteration by Equation (30), a curve computed

* In this model, the field profile is first computed with boundary motion neglected, and the interface material balance is then used to force the boundary position to be a function of time. The method is discussed in the Appendix of (6).

† If a great number of these calculations are necessary for solving a problem, use of a digital computer is suggested.

from the empirical form used by Hermans [Equation (34)] by assuming a diffusion coefficient of 1.6×10^{-6} sq. cm./sec. is shown. It is seen that the quasi steady model is a poor one for a penetration degree of about 25% and greater. Nevertheless, it may be seen that with even so poor an initial approximation, one iteration is sufficient to approximate the process fairly well.*

If one notes the time (Fourier group, Dt/R_o^2) of half penetration from Figure 2, the corresponding diffusivities may be computed from Equation (35) and the experimental value of k given by Hermans:

$$D \text{ (quasi steady)} = 0.62 \times 10^{-6} \text{ sq. cm./sec.}$$

$$D \text{ (first iteration)} = 1.32 \times 10^{-6} \text{ sq. cm./sec.}$$

Thus, although the quasi steady value is quite poor, the first iteration value approaches the measured value.

THE GROWTH OF SULFURIC ACID DROPLETS IN HUMID AIR

Description of Problem

The problem of the diffusion-controlled growth of a binary liquid droplet in a binary vapor is considered in this example. Specifically, attention is given to the growth of sulfuric acid droplets in the 500- to 1,000-μ diameter range in air saturated with water vapor at 25°C. The model considered allows for isothermal diffusion in both phases with equilibrium at the interface. Constant phase densities and diffusivities are assumed, and the liquid phase is considered to be stagnant. Bulk motion of the vapor phase toward the droplet as water is transferred is considered.

Diffusion in the Vapor

The differential equation for binary diffusion in the vapor may be written (*1*) as

$$D_V \frac{\partial^2}{\partial s^2}(w - w_o) + \left[\frac{2D_V}{s} - \epsilon\left(\frac{B}{s}\right)^2 \dot{B}\right] \frac{\partial}{\partial s}(w - w_o) = \frac{\partial}{\partial \theta}(w - w_o) \quad (41)$$

where w is the weight fraction of water vapor in the air, and w_o is the weight fraction far removed from the drop in the vapor phase (a constant). The boundary conditions are

$$(w - w_o) = 0 \quad \text{as} \quad s \to \infty \quad (42)$$

and

$$(w - w_o) = (w_B - w_o) \quad \text{at} \quad s = B(\theta) \quad (43)$$

The interface weight fraction w_B depends upon the phase equilibrium which shall be considered later. For the present, it is sufficient to note that w_B is a function of time.

If it is required that no air cross the phase boundary, continuity requires that

$$\frac{\partial}{\partial s}(w - w_o) = \frac{\rho_L}{D_V \rho_B}(1 - w_B)\dot{B} \quad \text{at} \quad s = B(\theta) \quad (44)$$

At the vapor concentrations of interest, the convective term in Equation (41) is negligible, so that the differential equation becomes linear and the quiescent phase procedure developed in (*1*) applies. As is usual in the case of the spherically-symmetrical diffusion equation, a certain amount of detail may be avoided by first making the substitution

* The waves in the result of the first iteration are presumably the result of some over and under corrections to the initial approximation and would be expected to become smoothed by succeeding iterations.

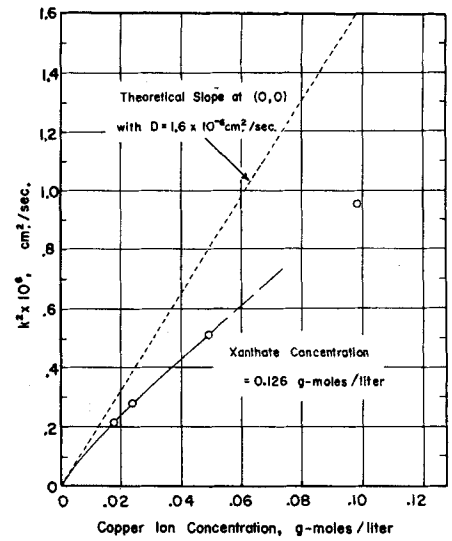

Fig. 1. Determination of the diffusion coefficient from the data of J. J. Hermans and the asymptotic form of the present theory.

$$u = s(w - w_o) \quad (45)$$

The resulting problem is stated as follows:

$$D_V \frac{\partial^2 u}{\partial s^2} = \frac{\partial u}{\partial \theta} \quad (46)$$

$$u = 0, \quad \theta = 0 \quad (47)$$

$$u = 0, \quad s \to \infty \quad (48)$$

$$u = B(w_B - w_o), \quad s = B(\theta) \quad (49)$$

$$\frac{\partial u}{\partial s} = (w_B - w_o) + \frac{B\dot{B}\rho_L}{D_V \rho_V}(1 - w_B), \quad s = B(\theta) \quad (50)$$

The auxiliary function, or solution to the auxiliary problem corresponding to Equations (46) through (51), is the simple one-dimensional source solution:

$$v = \frac{1}{2\sqrt{\pi D_V(\theta - \theta')}} \exp - \left[\frac{(s - s')^2}{4D_V(\theta - \theta')}\right] \quad (51)$$

By application of the boundary equations corresponding to Equations (I.7) and (I.13), one finds that†

$$\left(\frac{vG}{F}\right)_{B'} = B'(w_{B'} - w_o)\left(\frac{\partial v}{\partial s'}\right)_{B'} - v_{B'}\left[\frac{(w_{B'} - w_o)}{D_V} B'\dot{B}' + (w_{B'} - w_o) + \frac{\rho_L}{D_V \rho_V}(1 - w_{B'})\, B'\dot{B}'\right] \quad (52)$$

The solution, in terms of the original variables, is then

$$(w - w_o)\, s = D_V \int_0^\theta \frac{(w_{B'} - w_o)}{4\sqrt{\pi}[D_V(\theta - \theta')]^{3/2}} B'(s - B') \exp - \left[\frac{(s - B')^2}{4D_V(\theta - \theta')}\right] d\theta' - D_V \int_0^\theta \frac{1}{2\sqrt{\pi D_V(\theta - \theta')}} \left[\frac{B'\dot{B}'}{D_V}\left[(w_{B'} - w_o) + \frac{\rho_L}{\rho_V}(1 - w_{B'})\right]\right.$$

† A more detailed treatment of this problem may be found in reference (*6*).

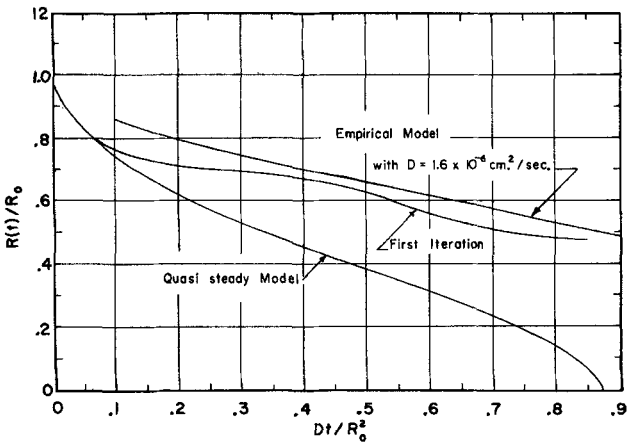

Fig. 2. Comparison of quasi steady, first iteration, and empirical models for boundary motion in run 7.

$$+ (w_{B'} - w_o) \Big] \exp - \Big[\frac{(s - B')^2}{4D_V(\theta - \theta')} \Big] d\theta' \qquad (53)$$

Equation (53) may be rearranged, whereupon for $s = B$ one has

$$(w_B - w_o)\, B = \int_0^\theta \frac{(w_{B'} - w_o)B'}{\sqrt{\pi}} \exp - \Big[\frac{B - B'}{2\sqrt{D_V(\theta - \theta')}} \Big]^2 \frac{d}{d\theta} \Big[\frac{B - B'}{2\sqrt{D_V(\theta - \theta')}} \Big] d\theta'$$

$$- \int_0^\theta \frac{\sqrt{D_V}}{2\sqrt{\pi(\theta - \theta')}} \Big[\frac{\rho_L(1 - w_{B'})B'\dot{B}'}{D_V\rho_V} + (w_{B'} - w_o) \Big] \exp - \Big[\frac{B - B'}{2\sqrt{D_V(\theta - \theta')}} \Big]^2 d\theta' \qquad (54)$$

Now it happens that for the ranges of variables of interest in this analysis, the left side of Equation (54) and the first integral term on the right side are quite small compared with either of the two terms making up the last integral. Therefore, Equation (54) degenerates into the following simple result:

$$B \frac{dB}{d\theta} \doteq \frac{D_V\rho_V(w_o - w_B)}{\rho_L(1 - w_B)} \doteq \frac{D_V\rho_V}{\rho_L}(w_o - w_B) \qquad (55)$$

While w_B is variable, it is always negligible compared with unity. It is of interest to note that this is the result that would be obtained by the quasi steady method.

Interface Equilibrium

It would be convenient from the mathematical point of view if the equilibrium relationship could be linearized. For the range of acid concentrations of interest here, this is not satisfactory. However, a good approximation is of the form

$$(w_o - w_B) = KW_B^2 \qquad (56)$$

where W_B is the weight fraction of acid in the liquid in contact with the vapor, and K is a constant. For example, the vapor pressure data of Stokes and Robinson (7) at 25°C. are well represented by Equation (56) for a pressure of 750 mm. Hg with $K = 0.053$.

When one combines Equation (56) with (55), the vapor diffusion and interface equilibrium may be summarized in the following equation:

$$B \frac{dB}{d\theta} = \frac{KD_V\rho_V}{\rho_L} W_B^2 \qquad (57)$$

Diffusion in the Liquid

The liquid phase diffusion problem may be stated, on the assumption that no acid escapes from the liquid phase, as follows:

$$D_L \frac{\partial^2 W}{\partial s^2} + \frac{2D_L}{s} \frac{\partial W}{\partial s} = \frac{\partial W}{\partial \theta} \qquad (58)$$

$$W = W_o, \quad \theta = 0 \qquad (59)$$

$$W = W_B, \quad s = B \qquad (60)$$

$$\frac{\partial W}{\partial s} = 0, \quad s = 0 \qquad (61)$$

$$\frac{\partial W}{\partial s} = \frac{-W_B\dot{B}}{D_L}, \quad s = B \qquad (62)$$

This problem is also of a form amenable to treatment by the quiescent phase procedure, but unfortunately the analysis does not reduce to a simple form as was the case for the vapor diffusion. It was found convenient to attack the liquid-phase problem numerically with the aid of the differential analyzer. The problem is conveniently transformed by

$$x = s/B \qquad (63)$$

and

$$t = \int_0^\theta D_L B^{-2}\, d\theta \qquad (64)$$

into

$$\frac{\partial^2 W}{\partial x^2} + \Big[\frac{2}{x} + \frac{x}{B} \frac{dB}{dt} \Big] \frac{\partial W}{\partial x} = \frac{\partial W}{\partial t} \qquad (65)$$

$$W = W_o, \quad t = 0 \qquad (66)$$

$$W = W_B, \quad x = 1 \qquad (67)$$

$$\frac{\partial W}{\partial x} = 0, \quad x = 0 \qquad (68)$$

$$\frac{\partial W}{\partial x} = \frac{-W_B}{B} \frac{dB}{dt}, \quad x = 1 \qquad (69)$$

Also, Equation (57) becomes

$$\frac{1}{B} \frac{dB}{dt} = K \frac{D_V\rho_V}{D_L\rho_L} W_B^2 \qquad (70)$$

Once again, a convenient simplification results for the problem at hand. The nonlinear term in Equation (65) may be neglected with substantially no error.* When one takes into account this simplification and writes

* Order of magnitude simplifications such as these often are not recognized a priori but are quickly discovered as soon as one begins to scale the problem for machine solution.

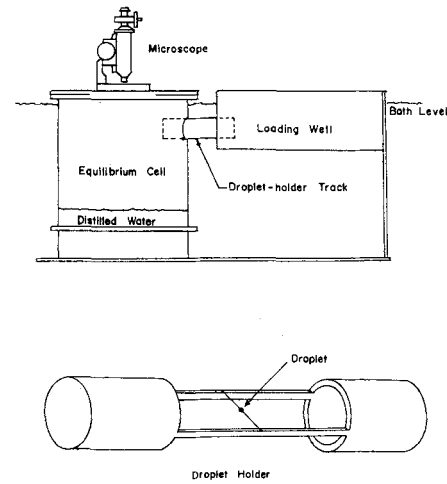

Fig. 3. Experimental apparatus.

$$U = Wx \tag{71}$$

the problem becomes

$$\frac{\partial^2 U}{\partial x^2} = \frac{\partial U}{\partial t} \tag{72}$$

$$U = W_o x, \quad t = 0 \tag{73}$$

$$U = W_B, \quad x = 1 \tag{74}$$

$$U = 0, \quad x = 0 \tag{75}$$

$$\frac{\partial U}{\partial x} = W_B - \frac{W_B}{B}\frac{dB}{dt}, \quad x = 1 \tag{76}$$

$$\frac{1}{B}\frac{dB}{dt} = K\frac{D_V \rho_V}{D_L \rho_L} W_B^2 \tag{77}$$

The problem posed by Equations (72) through (77) may be reduced to a set of simultaneous ordinary differential equations by replacing derivatives in x by finite-difference approximations in a six-interval, second-order approximation scheme. This set of equations, depending upon the single parameter β, where

$$\beta = KW_o^2 \frac{D_V \rho_V}{D_L \rho_L} \tag{78}$$

may then be solved on the differential analyzer to obtain the group $(1)/(B)\ (dB)/(dt)$ as a function of t. Solution in terms of the original variables is then found as

$$\left(\frac{B}{B_o}\right)^2 = \exp\left[\, 2\int_0^t \frac{1}{B}\frac{dB}{dt}\, dt \,\right] \tag{79}$$

and

$$\frac{D_L \theta}{B_o^2} = \frac{D_L}{B_o^2}\int_0^t \frac{B^2}{D_L}\, dt = \int_0^t \left(\frac{B}{B_o}\right)^2 dt \tag{80}$$

EXPERIMENTAL

The rates of growth of small, single droplets of sulfuric acid in an environment of air saturated with water vapor at 25°C. and atmospheric pressure were measured by means of the apparatus shown in Figure 3.

The entire apparatus, with the exception of the fiber on which the droplets were suspended, was constructed of Lucite. The exposure chamber itself consisted of a cylinder having an outside diameter of 6.0 in. This cylinder was sealed permanently at the bottom by a plate. A top plate was sealed temporarily by means of a film of low vapor-pressure stopcock grease to facilitate changing the water in the cell and cleaning the viewing plate.

A tube having an outside diameter of 1.0 in. connected the exposure cell and the loading well. This tube served as a track for the droplet-holding apparatus shown in Figure 3.

The droplet holder consisted of a tube which was finished so that it fit snugly into the track tube but could be moved smoothly in or out of the cell when lubricated with stopcock grease. Both ends of this tube were closed so that the exposure cell was sealed from the room air when the droplet holder was in the loading position (in the loading well) and when it was in the exposure position (in the cell).

The droplets were suspended on a single fiber of glass wool which was attached to the moveable cylinder as indicated in Figure 3. These fibers were prone to breakage, so that several were used during the course of the experiments. Thus, while their diameters varied, they were all in the 10- to 15-μ range.

The entire apparatus was immersed in a constant-temperature bath which was maintained at 25 ± 0.2°C. The cell was charged to a depth of about 1 in. with double-distilled water, and in each case several hours were allowed for the chamber to come to equilibrium before any runs were made.

A microscope of sixty-power magnification was placed atop the exposure cell. The eyepiece of this instrument contained a calibrated graticule which was used to measure the diameter of a growing droplet at selected intervals of time. The smallest scale division corresponded to 2.54μ.

Illumination was provided by a microscope lamp situated above the bath and directed toward the floor of the exposure chamber, which was painted white (on the bath side). The droplets appeared as sharply defined dark circles against the light background.

The technique of forming and exposing a droplet was as follows. The droplet was formed at the end of a capillary tube containing the acid solution, the tip of which was of such size that a small droplet could be formed with difficulty when pressure was applied by mouth to the large end. The capillary tube was then drawn across a fine filament drawn from glass cane. This intermediate holder tapered from a diameter of about 100μ down to substantially nil. The latter was then drawn across the final glass wool fiber, thus sliding the droplet toward the small end of the intermediate holder until it attached itself to the final holder. The holding apparatus was then slid immediately into the exposure cell, the time was noted, and the diameter observations were begun.

It was not possible, by means of this technique, to select a droplet of a particular diameter. It should also be noted that several attempts were usually required in order to form and transfer a droplet successfully.

Runs were made for droplets initially containing 14.9, 30.2, 46.0, and 62.1 wt. % sulfuric acid. These data are tabulated in (6). Results of a typical run are presented graphically in Figure 4.

COMPARISON OF MODEL WITH EXPERIMENT

It may be noted from Figure 4 that there is a time lag of about 5 min. before the droplet begins to grow. This is attributed to an exposure cell entrance effect. To assure that the growth rates considered are controlled by the quiescent, saturated environment of the exposure cell, the first 5 min. of cell time are completely ignored in comparing model with experiment. That is, conditions after 5 min. of exposure are, in each case, taken as initial conditions of the model.

The model of the process, it is recalled, depends upon the single constant parameter β, defined by Equation (78). Assignment of a value of β for a particular set of conditions is a problem of considerable difficulty for the following reasons. While one should be able to make a reasonable estimate of D_V, ρ_V, and ρ_L, W_o being known, estimation of the empirical equilibrium constant K and the liquid-phase diffusion coefficient D_L is much more difficult.

In the case of K, the exposure cell was thermostated at 25 ± 0.2°C., and the vapor phase may reasonably be assumed to be at this temperature; however, the liquid phase must, on the other hand, be at some higher temperature, determined by the energy balance. If it is as-

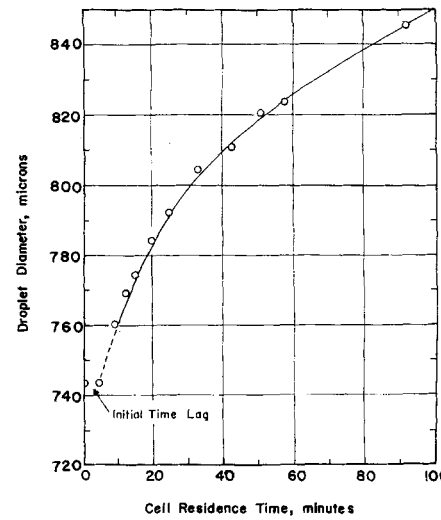

Fig. 4. Growth curve for an acid droplet (Run 1).

sumed that thermal relaxation is rapid with respect to the mass diffusion, it follows that the droplet ought to assume some relatively steady temperature early in the process. If this were correct, a constant value of K should suffice, but not the value for 25°C.

The value of K is extremely sensitive to temperature. For example, it may be concluded from an inspection of vapor pressure data at various temperatures [see Perry (8)] that the growth process would be entirely reversed for a droplet containing 15% acid, if the temperature were to rise about 2°C. The precision of vapor pressure data as a function of temperature does not seem to justify a detailed calculation of these thermal effects.

Determining a value for the liquid diffusivity is also difficult. The available data are contradictory, and in general the concentration dependence of D_L is not well established.

In view of these practical problems, it seems appropriate to abandon any atttempt at a completely theoretical calculation in favor of a semiempirical one. The approach is to let any point of the experimental growth curve determine the value of β for the conditions in question. With this attitude, one might expect that if the model can be matched with experimental results at one point by suitable choice of β, it would then match at all other points if the diffusion model were correct.

Results of this matching procedure are summarized in Figure 5, where the curves are computer solutions of the model for the values of β shown. From this figure, it is clear that the model gives growth curves which are of the correct shape, and that the agreement is good once β is determined. It should be pointed out that in order to plot the experimental data on these coordinates, it was necessary to assume a value for the liquid phase diffusion coefficient. The value assumed was 2×10^{-5} sq. cm./sec., which is hardly more than a guess, and may be considered as simply a dimensional scaling factor for the time axis in this figure.

Figure 6 shows the behavior of the surface concentration predicted by the model, which may be of interest.

Although β cannot be calculated easily from first principles, it was found empirically that this parameter is well correlated with the initial droplet concentration. The values of β required to fit the data of Figure 5 are closely predicted by the empirical equation

$$\beta = 0.00372 \exp (4.60\, W_o) \qquad (81)$$

SUMMARY AND CONCLUSION

The problem of phase boundary motion in diffusion-controlled processes has been considered, and three general methods of solution have been shown. The first of these methods was developed by means of a Riemann integration of the diffusion equation. This procedure is suitable only for the case of the linear diffusion equation (no convection) but in this case the integro-differential equation describing the boundary motion can be written down immediately in terms of the definite integral of a Green's function.

For problems involving phases of significantly different densities in which bulk motion of one phase with respect to the other must be accounted for, an alternate analytical procedure, based upon the method of intermediate integrals, was presented. This method depends upon a successful choice of a transformation of variables at the outset and offers no guarantee of success. Where it is successful, results are likely to be obtained in a more convenient form than by application of the first method. All closed-form solutions known to the authors may be obtained by this method, and it may be considered to be a generalization of the special methods used individually by the several analysts who originally produced these solutions.

Finally, a numerical procedure involving finite-difference approximations in conjunction with the differential analyzer was offered. This procedure will yield numerical solutions to all of the problems considered in this work to a degree of accuracy governed principally by the amount of computing equipment used.

The methods were applied, sometimes in combination, to the problems of the evaporation from a plane interface, the penetration of a reaction front into a cylindrical fiber, and the growth of a spherical droplet. In the last two applications, the models were shown to be of use in interpreting actual experimental data for the problems concerned.

In conclusion, it is believed that the present work has organized the approach to the moving-boundary problem and presented several general methods of solution.

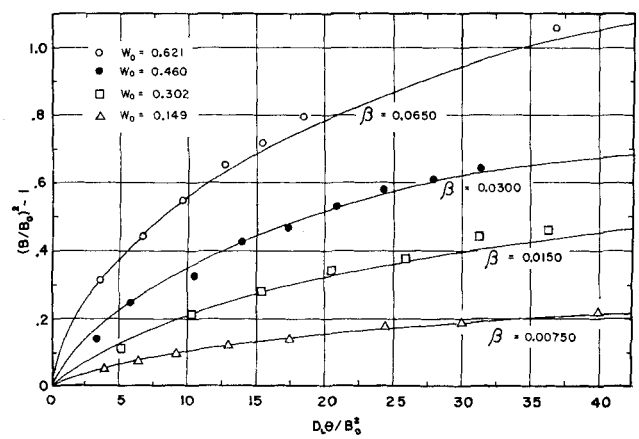

Fig. 5. Comparison of model and experiment.

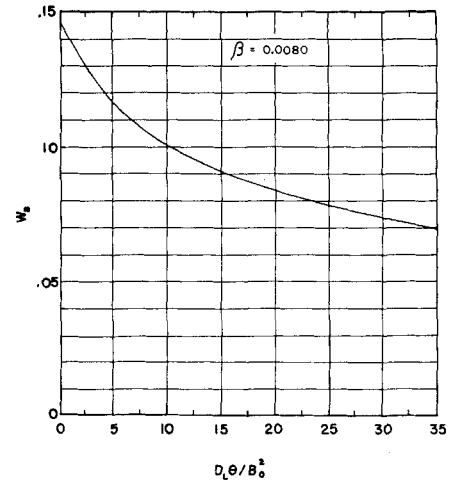

Fig. 6. Typical behavior of surface acid concentration.

NOTATION

- a = molar concentration of copper ion in solution surrounding fiber
- B = dimensionless boundary position in fiber
- B = dimensional boundary position in droplet
- b = molar concentration of xanthate in fiber
- c = molar concentration of copper ions in metal xanthate
- D = diffusivity of copper ions through metal xanthate
- D_F = value of D computed by Fujita (5)

D_H = value of D computed by Hermans (3)
D_L = diffusivity of sulfuric acid in water
D_V = diffusivity of water vapor in air
F = function symbol
G = function symbol
K = empirical equilibrium constant in droplet problem
k = an empirically-determined parameter in the fiber problem
R = dimensional boundary position in fiber
R_o = radius of cylindrical fiber
r = dimensional radial position in fiber
s = dimensionless radial position in fiber
s = dimensional radial position in droplet
T = a parameter corresponding to the time required for penetration to the center of fiber
t = dimensional time in fiber problem or in droplet problem
U = a transformed dependent variable in the droplet problem
u = dimensionless concentration in fiber problem
u = a transformed dependent variable in the droplet problem
v = auxiliary function
W = weight fraction sulfuric acid in water
w = weight fraction water vapor in air
x = dimensionless position in droplet

Greek Letters

β = phase growth parameter in droplet problem
ϵ = density function, $(\rho_V - \rho_L)/\rho_V$
θ = dimensionless time in fiber problem
θ = dimensional time in droplet problem
λ_n = an eigenvalue
ρ_L = liquid phase density
ρ_V = vapor phase density
ϕ = function symbol

LITERATURE CITED

1. Griffin, J. R., and D. R. Coughanowr, *A.I.Ch.E. Journal*, **11**, No. 1, p. 133 (1965).
2. ———, *ibid.*, p. 151.
3. Hermans, J. J., *J. Colloid Sci.*, **2**, 387 (1947).
4. Hermans, P. H., "Physics and Chemistry of Cellulose Fibers," Elsevier, New York (1949).
5. Fujita, Hiroshi, *J. Chem. Phys.*, **21**, 700 (1953).
6. Griffin, J. R., Ph.D. thesis, Purdue University, Lafayette, Indiana (1963).
7. Stokes, R. H., and R. A. Robinson, *Ind. Eng. Chem.*, **41**, 2013 (1949).
8. Perry, J. H., "Chemical Engineers' Handbook," 3 ed., McGraw-Hill, New York (1950).

Manuscript received August 30, 1963; revision received September 22, 1964; paper accepted October 1, 1964.

Effect of the Equilibrium Relationship on the Dynamic Characteristics of Distillation Column Sections

C. MICHAEL MOHR

Massachusetts Institute of Technology, Cambridge, Massachusetts

The dependence of the dynamic characteristics of distillation column sections on the shape of the equilibrium relationship and the number of plates comprising the section is discussed. Dynamic characteristics, valid near the steady state operating condition, were obtained for simple column sections separating binary mixtures by a straightforward calculation with a digital computer. Sections with concave downward equilibria respond significantly more slowly than comparable sections with linear equilibria. Sections with concave upward equilibria respond faster. This behavior is explained in terms of the internal recycle within the section. The rate of propagation of a disturbance from end to end in the section is only weakly influenced by the shape of the equilibrium relationship.

A considerable body of literature exists concerning the control of distillation columns. The two major areas of investigation are the behavior of distillation systems during start up and the control of systems operating at steady state and perturbed by small changes in operating conditions. System dynamics and control loop design have been studied in each area. The recent literature has been well summarized by Rosenbrock (*1, 2*) and by Archer and Rothfuss (*3*). This paper deals with the dynamics of systems operating at a steady state condition.